SOLAR CORONA SEISMOLOGY

JOSE LUIS BALLESTER
Departament de Física, Universitat de les Illes Balears, E-07122 Palma de Mallorca, SPAIN

Abstract: The presence of oscillations in solar coronal structures has been known for more than seventy years. Observational reports about the presence of oscillatory motions in solar filaments go back to 1930 while in the case of other coronal structures (loops, plumes, etc) direct evidence has been recently obtained thanks to the detailed observations made by SoHO and TRACE. Due to these satellites, as well as to ground-based observations, evidence of magnetohydrodynamic (MHD) waves in the solar corona has risen dramatically. MHD coronal seismology provides with an indirect path to determine the physical conditions and parameters of the solar corona [coronal magnetic field, transport coefficients (viscosity, resistivity, thermal conductivity, etc.), heating function, filling factors] which are difficult to measure accurately. In essence, it is similar to the acoustic diagnostic of the solar interior (Helioseismology) and to MHD spectroscopy used to determine physical parameters of laboratory plasmas. In spite that there are many solar coronal structures in which oscillations have been detected (prominences, loops, plumes, coronal holes, etc.), in the following we will concentrate in prominences and coronal loops trying to summarize part of our current knowledge about their oscillations as well as about the theoretical models developed to explain those oscillations in terms of MHD waves.

1 Introduction

Observational reports about the presence of oscillatory motions in solar filaments go back to 1930 [1]. During many years, up to 1960, all these reports described oscillations of filaments induced by a disturbance coming from a flare, a phenonemon which was called "winking filaments". It was suggested that the exciter of these oscillations was a wave, caused by the flare, which disturbs the filament and induces damped oscillations. This hypothesis was confirmed by [2] whose works permitted the observation of the propagation of the disturbance (Moreton wave) from the flare to the filament. Nowadays, thanks to the use of ground and space-based facilities those exciters have been properly identified as

Moreton and EIT waves, however, in spite that this phenomenon is well known for more than fifty years few theoretical studies explaining the full phenomenon have been undertaken [3, 4, 5].

On the other hand, from observations performed by ground-based telescopes we know from long time ago [6] that quiescent prominences display small-amplitude oscillations detected, mainly, through the periodic Doppler shift of spectral lines. In the last years, on-board SoHO instruments [7, 8, 9, 10] as well as high-resolution observations performed by ground-based telescopes (SST, La Palma) have provided us with numerous evidences of prominente oscillations [11]. Those oscillations appear in prominences [12] as well as in filaments and, in this case, they seem to be related to the filament's fine structure displayed in high-resolution observations [13]. Furthermore, some of these observations have pointed out the damping or amplification of oscillations [12, 13, 14], the existence of standing or propagating waves [12], and have allowed to obtain some estimations of the wavelength and phase velocity of propagating waves in solar prominences [12, 15].

SoHO and TRACE satellites have also provided us with a lot of evidences about the presence of oscillations in coronal loops. From the 1960s we had already indirect evidences of oscillations coming from radio observations and coronal emission lines, but SoHO and TRACE have observed, or obtained direct evidences, of: Transversal oscillations in coronal loops [16, 17, 18] and their short time damping; of compressive waves in short and long coronal loops [19, 20, 21]; of quasi-periodic oscillations of the Doppler shift and intensity of the iron XIX and XXI emission lines in coronal loops [22, 23] and their damping, etc.

Theoretical studies of oscillations and MHD waves in the solar corona started more than twenty years ago, before many of the above mentioned observations, and the interest of their study lies in their potencial relationship with the coronal heating problem. [24] and [25], gave a tentative explanation of the indirect evidences of coronal oscillations in terms of standing or impulsive MHD waves in coronal loops considered as straight and infinite magnetic flux tubes. Nowadays, the theoretical range of periods is well covered by the time resolution available in ground-based telescopes and in on-board satellite instruments and this fact, together with other observational details, allows the attribution of theoretical counterparts (modes of oscillation) to observations. Then, oscillations observed in coronal loops have been interpreted in terms of MHD waves, and different MHD modes responsible for those oscillations have been identified [26, 27, 28, 29, 30]. The identification of these modes is the key for the local seismology of the solar corona and it has allowed preliminary estimations of the magnetic field and plasma β in coronal loops [28] and solar prominences [31]. The main goal of the local seismology of the solar corona is to use the oscillations detected in coronal

structures, and their interpretation in terms of MHD waves, as a tool to perform a diagnostic of the physical properties of those structures and in the near solar corona. For instance, the coronal magnetic field in the magnetic structures and surroundings, the transport coefficients (viscosity, resistivity, thermal conductivity, .), etc. Philosophically, the method is similar to the seismic sounding of the Earth performed by geophysicists using seismic waves or to the acoustic diagnostic of the Sun's interior (Helioseismology), and it has been also used in laboratory plasmas (JET), under the name MHD spectroscopy, for more than a decade [32].

2 Prominence Oscillations

2.1 Flare-Initiated Filament Oscillations

The phenomenon of "winking filaments" was already reported by [1]. This name derives from the fact that during the course of the oscillations, the filament becomes visible in the Hα image when the prominence is at rest, but when its line-of-sight velocity is sufficiently large, the emission from the material falls outside the bandpass of the filter and the prominence becomes invisible in Hα . The resulting optical effect gave rise to coining the term "winking filament". [2] used a refined photographic technique which permitted the observation of the propagating perturbation, with velocities in the range 500 km s^{-1}-1500 km s^{-1}, and pointed out clearly that this kind of oscillations arise when the whole prominence is shaken by a wave impinging on it. [33] studied 11 winking filaments and derived oscillatory periods between 6 and 40 minutes. They reported that there seemed to be no correlation between the period and the filament dimensions, the distance to the flare or its size. In addition, a single filament perturbed by four flares during three consecutive days oscillated with essentially the same frequency each time. It was then suggested that prominences possess their own frequency of oscillation. Another interesting property of these flare-initiated oscillations is that perturbations were typically present for two to four periods before being damped. Recently, and thanks to space and ground-based observations, new observations about winking filaments have been published and the exciters have been identified. [34] studied the relationship between Moreton and EIT waves produced by an X-class flare on 1997 November 4 finding that the Moreton wave was responsible for the oscillations, with a period of 20 minutes, of a quiescent filament located as far as 800,000 km from the flare site. Furthermore, a prominence eruption was also observed along the direction of propagation of the Moreton wave but closer to the flare site. [35] have analysed the effects on filaments caused by an EIT wave produced by a GOES X2.3 flare on 2001 April 10.

The EIT wave triggered the oscillations of four filaments located in different regions of the Sun and in one of the cases a period of oscillation of 28 minutes was observed. Although in most of the observed flare-induced filament oscillations the material undergoes vertical oscillations, [5] reported one case of horizontal oscillations in a limb prominence on August 24, 1953. In this sense, [36] reported the periodic motions along a filament produced by a disturbance coming from a sub-flare in the neighbourhood. The motions are clearly seen in Hα and the displacement of the material can be measured. From the time evolution of the positions of the material, a velocity curve can be derived and the best fit to one of those curves gives an initial displacement of 7.0×10^4 km, a period of 80 minutes, a damping time of 210 minutes and a maximum velocity of 92 km$\cdot s^{-1}$.

From the theoretical point of view, models fully explaining the winking filament phenomenon are lacking. To explain the vertical motions, [3] suggested that the disturbance coming from the flare is propagated along the magnetic field and when it arrives to the filament pushes the material down. [4] proposed a model which analysed the vertical motions in terms of harmonically damped oscillations. The restoring force was provided by the magnetic tension while the damping was due to coronal viscosity. Using this model, [4] was able to calculate the strength of the vertical component of the magnetic field in the prominence. Later, [5] proposed a similar model to explain the horizontal oscillations but, in this case, the damping was provided by the emission of acoustic waves.

2.2 Small Amplitude Oscillations: Observational Background

They are observed in prominences and filaments with velocity amplitudes much smaller than those of flare-induced oscillations. The detected peak velocity ranges from the noise level (down to 0.1 kms^{-1} in some cases) to 2–3 kms$\cdot s^{-1}$, although larger values have also been reported [12, 14, 37]. On the other hand, it now appears well established that small amplitude, periodic changes in solar prominences do not normally affect the whole object at a time, but are of local nature instead. Observational studies have revealed a great diversity of characteristic periods ranging from smaller than 1 minute up to 90 minutes. Two-dimensional, high-resolution observations of a limb-prominence [12, 14] have allowed to construct Doppler, period, damping time and wavevector maps and to obtain interesting information about this kind of oscillations in prominences. For instance, [12] have reported the existence of large regions with periodic Doppler velocity oscillations having similar periods, around 75 minutes, noticing also that the oscillatory amplitude tends to decrease in time in such a way that the periodicity totally disappears after a few periods. Reliable values of the damping time, τ,

have been derived by [14] and [12] after fitting a sinusoidal function multiplied by a factor $\exp(-t/\tau)$ to different Doppler velocity time series. The values of τ thus obtained are usually between 1 and 3 times the corresponding period, and large regions of the prominence display similar damping times. Also, [12] reported the presence, along two selected paths in the prominence region, of a plane propagating wave as well as an standing wave. The plane wave propagate in opposite directions with wavelengths of $67,500$ and $50,000$ km and phase speeds of 15 km$\cdot s^{-1}$ and 12 km$\cdot s^{-1}$, while in the case of the standing wave the estimated wavelength is of $44,000$ km and the phase speed of 12 km$\cdot s^{-1}$. Furthermore, the analysis has identified the existence of a wave generating region pointing out that oscillations are locally excited.

Related to small amplitude oscillations in filaments, recent two-dimensional, high-resolution observations of filaments [13, 38] have provided with interesting information about filament's structure and oscillations. The analysis of these observations suggests that the width of thin threads forming the filaments is $\leq$ 0.34 arc sec, and that the absorbing plasma is continuously flowing along the thread structure with velocities 15 ± 10 km$\cdot s^{-1}$. On the other hand, when the central part of a polar crown filament is covered with a large number of parallel, thin slices and the average Doppler signal of each slice is plotted as function of time, a significant periodicity at 26 minutes appears, but it is strongly damp after 4 periods while the phase is maintained over this large filament area. This confirm earlier conclusions [39, 40] that individual fibrils or groups of fibrils may oscillate independently with their own periods, which range between 3 and 20 minutes. More extense observational information about small amplitude oscillations in prominences and filaments can be found in [41, 42, 11, 43].

2.3 Small Amplitude Oscillations: Theoretical Models

Oscillations of Slab Prominence Equilibria

An in-depth study of the oscillatory modes of the Kippenhahn & Schlüter prominence model was undertaken by [44]. In this work it was noted that the three MHD modes possess different velocity orientations, with the fast mode characterised by vertical motions, the Alfvén mode by motions along the filament long axis and the slow mode by plasma displacements parallel to the equilibrium magnetic field, which in this configuration is practically horizontal and transverse to the prominence. The immediate consequence of this association between modes and velocity polarisation is that periodic variations in the Doppler shift are more likely to be detected in filaments near the disk centre for fast modes and in limb prominences for Alfvén and slow modes, depending on the orientation of the

prominence with respect to the observer. [45] were the first to acknowledge the importance of including the surrounding corona into the prominence equilibrium solution by representing a prominence as a cool and dense plasma slab embedded in a coronal environment. The influence of gravity was neglected and so the plasma variables (temperature, pressure and density) are uniform both in the prominence and in the coronal region. The magnetic field is also uniform and, for the sake of simplicity, assumed transverse to the prominence. After perturbing this simple equilibrium configuration, analytical solutions for the velocity components can be obtained. Attending to the characteristic wavenumbers of these solutions, [45] created the distinction between internal and external modes. According to these authors, the former group of modes arises principally from the magnetoacoustic properties of the plasma slab, although these modes are somewhat influenced by the external material because of the presence of free interfaces between the prominence and corona. External modes are present, however, even in the absence of the prominence plasma but are modified because of the introduction of this cool, dense slab. Moreover, Joarder and Roberts also derived approximate expressions for the frequency of slow and fast modes in the infinite wavelength limit and appreciated that, for some modes, ω strongly depends on the length of magnetic field lines.

Oliver et al. [46] provided with more insight into the nature of internal and external modes while using a modified, non-isothermal Kippenhahn-Schlüter solution [47] consisting of an isothermal prominence surrounded by an isothermal corona. The presence of the prominence (coronal) region thus provides "physical support" for the existence of internal (external) modes. A clear distinction then arises between the two types of modes, although it turns out that the fundamental mode is internal and external at the same time, since it "survives" both when the prominence and the corona are eliminated. For this reason, this mode with mixed internal and external properties was called hybrid by [46] and later string by [45]. From [46] it also appears that the amplitude of perturbations in the prominence is rather small for external modes and so it was postulated that they would probably be difficult to detect in solar prominences and that the reported periodic variations are produced by the hybrid and internal modes. In addition, the frequency of internal modes is showed to depend on prominence properties only, while that of hybrid and external modes depends on other physical variables such as the length of field lines.

In a prominence, magnetic lines are actually oriented at a rather small angle (around 20^{o}) with the prominence axis. [48] took this observational fact into account by adding a longitudinal magnetic field component to the equilibrium and considering also longitudinal propagation. The resulting dispersion diagram displays a very rich mode structure with plenty of mode couplings, which antici-

pates the complex nature of actual prominence oscillations and, probably, there are no characteristic oscillatory directions associated to the various modes.

Some attempts to explain the damped oscillations reported by [12, 14] have been also made. [49] have considered an slab-like prominence and have removed the adiabatic assumption by considering a full energy equation including optically thin radiation, thermal conduction and heating. The results indicate that the effect of thermal conduction is negligible in prominences and that the balance between radiative losses and heating is responsible for the damping of magnetoacoustic slow modes. Furthermore, the damping time depends on the radiation time, becoming longer or shorter than the period when the radiation time is modified. However, there are other possible mechanisms that can provide with an explanation for the observed damping of prominence oscillations such as wave leakage [50, 31, 51], resonant absorption [52] and ion-neutral collisions [53, 54].

Oscillations of Prominence Fibrils

The first theoretical investigation of periodic prominence perturbations taking into account the prominence fine structure was performed by [55]. In essence, the equilibrium is similar to that in [56] with the difference that the plasma slab has a limited height, so the configuration is reminiscent of a thin thread with finite width and length. Nevertheless, the fibril is infinitely deep since the equilibrium configuration is invariant in one direction, namely along the longitudinal prominence axis of the original equilibrium used by [56] from which this fibril structure follows. To further simplify the problem, the influence of plasma pressure is neglected (zero-β limit) and consequently the slow mode is absent. Thus, one is left with the Alfvén and fast modes and the main conclusion of this work is that, since the equilibrium structure contains two regions with uniform (and different) temperatures, internal, external and hybrid modes are also supported. Later, [50] performed a more in-depth analytical and numerical study of the same configuration. The main conclusions that can be extracted from their study are that prominence fibrils can only support a few modes of oscillation, those with smaller frequency, since high harmonics cannot be trapped inside the thin loop, and that the spatial structure of the fundamental even and odd kink modes is such that the velocity amplitude outside the fibril takes large values over long distances, although when longitudinal propagation is included the confinement of the velocity is slightly improved [51]. An interesting issue concerning these results is that most of the energy seems to be pumped out into the corona, so that fibrils would actually oscillate in groups rather than individually. This wave leakage could give a damping mechanism for fast mode oscillations which,

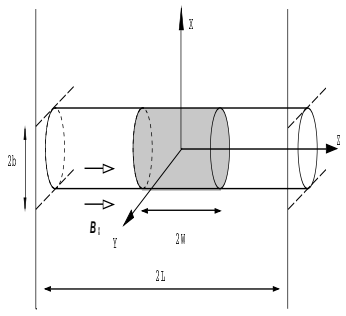

Figure 1: Sketch of the equilibrium configuration. The grey zone represents the cold part of the loop, i. e. the prominence. The density in the prominence region is ρ_p, in the evacuated (coronal) part of the loop, ρ_e, and in the coronal environment, ρ_c. The magnetic field is uniform and parallel to the z-axis, and the whole configuration is invariant in the φ-direction. Adapted from [31].

working together with some other mechanism affecting slow modes, can help to explain the time damping of prominence oscillations.

Díaz et al. [31] analysed the fast MHD oscillations of a more realistic model for the prominence fibril structure. The considered equilibrium assumes a straight cylindrical flux tube with a cool region representing the prominence, which is confined by two symmetric hot regions (Figure 1). For a thin, realistic fibril the properties of the eigenfrequencies and eigenmodes found in this case change completely with respect to those found in [31]. For instance, the fundamental sausage mode ($m = 0$) and its harmonics are always leaky since their frequency does not lie below the cut-off frequency. Therefore, if one of these modes is excited in the prominence fibril, its energy is quickly transferred to the coronal environment and the cold plasma stops oscillating. However, for all other modes ($m > 0$), i.e. those having angular dependence, at least the fundamental mode lies below the cut-off frequency. Hence, if any of these modes is excited the oscillatory energy in the prominence plasma does not vary in time. Moreover, as the density ratio between the prominence and the coronal medium ($\rho_{\rm p}/\rho_{\rm c}$) is increased, the frequency of other harmonics may move below the cut-off and so the structure may support a higher number of oscillatory modes. Regarding the spatial structure of perturbations, in cylindrical geometry the modes are always confined in the dense part of the flux tube (Figure 2). Therefore, an oscillating cylindrical fibril is less likely to induce oscillations in its neighbouring fibrils, unless they are very close. Anyway, this does not diminish the interest of

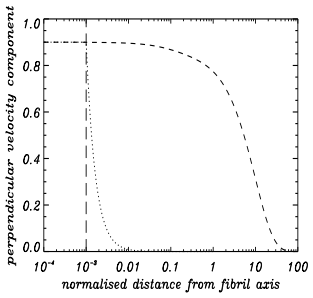

Figure 2: Sketch of a cut of the perturbed velocity component v_x in Cartesian geometry (dashed line) and v_r in cylindrical geometry (dotted line) in the direction across the fibril centre. These solutions correspond to the fundamental kink mode in a prominence fibril with parameters $\rho_e/\rho_c = 0.6$, $\rho_p/\rho_c = 200$, $W/L = 0.1$ and $b/L = 0.01$. The vertical long dashed line marks the fibril boundary. Adapted from [31].

studying interactions between fibrils in multifibril systems.

Díaz et al. [57] have studied multifibril systems in cartesian geometry. The equilibrium model consists of a collection of 2D fibrils separated a distance $2c$ (which is the relevant parameter), which are modeled as in [comprobar] [31]. The loop is anchored in the photosphere, so its footpoints are subject to line-tying conditions. Finally, the plasma is permeated by a uniform magnetic field directed along the prominence fibril (Figure 3). Because gravity is neglected, all other physical variables (ρ, T and p) are also uniform in each of the three regions, and invariance in the y-direction has been assumed. Following this approach, inhomogeneous filaments have been constructed and the different fibril density ratios represent the inhomogeneity in density of a real prominence, i. e. a different Alfvén velocity for each fibril, and the separation between fibrils has been chosen randomly within the realistic range (Figure 4). When the separation between fibrils is small, there is a strong interaction between them since the perturbation can easily overcome the separation and, as a result, there is only one even non-leaky mode: that one producing that all the fibrils oscillate in phase. The frequency dependence on the fibril separation (named $c_{\rm ref}$), while keeping the rest of the parameters values constant, can be studied and in the limit $c_{\rm ref} \to \infty$, the structure and the frequencies of each fibril oscillating alone are recovered, while for small values of $c_{\rm ref}$ all the non-phase oscillating modes are leaky, and only the mode described before remains having a slightly smaller frequency than

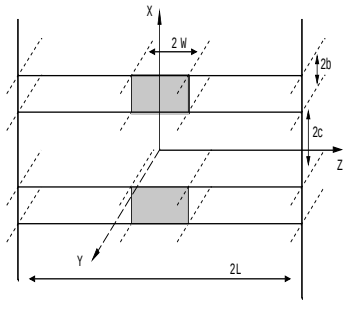

Figure 3: Sketch of the equilibrium configuration. The grey zone represents the cold part of the loop, i. e. the prominence. The density in the prominence region is $\rho_{\rm p}$, in the evacuated (coronal) part of the loop, $\rho_{\rm e}$, and in the coronal environment, $\rho_{\rm c}$. The magnetic field is uniform and parallel to the z-axis, and the whole configuration is invariant in the y-direction. Adapted from [57].

in the case of the single dominant fibril mode (Figure 5). Therefore, for realistic values of the separation between fibrils, the multifibril system would oscillate in phase, with similar amplitudes and the same frequency (smaller than the eigen-frequency of the more dense fibril). These results, although derived in cartesian geometry, strongly agree with the observations of filament thread's oscillations reported by [13] about the constancy of the oscillatory phase over large areas of the filament having the same period of oscillation. Further information about theoretical models for small amplitude oscillations in prominences and filaments can be found in [30, 58, 59].

3 Coronal Loops Oscillations

3.1 Fast kink-mode oscillations

In 1998, the imaging telescope onboard TRACE detected damped transversal oscillations of coronal loops located within an active region [16, 17, 60]. Following this observation, other observations of transversal oscillations in coronal loops have been obtained with TRACE [61, 62, 63]. In most cases, oscillations are triggered by a nearby flare [64] and produce transversal loop motions. These oscillations have been interpreted as standing fast kink magnetohydrodynamic modes of the loops since they produce transversal displacements of the axis. The

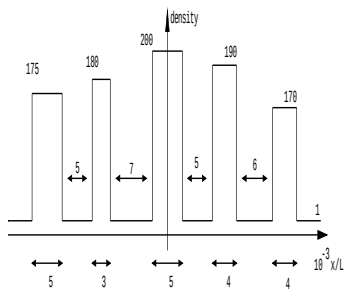

Figure 4: Sketch of a cut in the direction $z = 0$ of the normalised density profile (ρ/ρ_c) in the case of an inhomogeneous multifibril system. Between and under the fibrils the non-dimensional separation and width are given, respectively. Adapted from [57].

average period of the oscillating loops is 321 ± 140 s while the average damping time is 580 ± 385 s

An interesting feature of the amplitude of these oscillations is that it is strongly damped with a damping time of the order of a few periods. The interpretation of the physical mechanism that produces these oscillations is of great interest since it can provide with indirect information about the coronal plasma and in addition it can shed new light on the role of wave heating in coronal loops. Several mechanisms of wave damping have been proposed, the most popular ones being phase mixing and resonant absorption. Ofman and Aschwanden [65] used observational data to calculate the scaling laws of different damping mechanisms and suggested that phase mixing can be favored in front of resonant absorption. However, phase mixing in the simple form derived by [66] and used to calculate the damping times indicates that the magnetic Reynolds number (R_m) should be five or six orders of magnitude smaller than the classical coronal value ($R_m \approx 10^{12}$) to reproduce the damping times of the oscillating loops. It has been suggested that such a small anomalous Reynolds numbers could be produced by turbulence. On the other hand, [67] pointed out that the damping of kink oscillations by resonant absorption gives a consistent explanation of the rapid decay of the observed coronal loop oscillations if the transverse inhomogeneity length-scale is allowed to vary from loop to loop. This mechanism was used by [68] to show that the damping times for the kink mode oscillations are in agreement with the observations and that resonant absorption can provide with a new diagnostic tool for the density contrast in loops, although [69] have calculated the quasi-modes in fully non-uniform one-dimensional equilibrium models and have found that

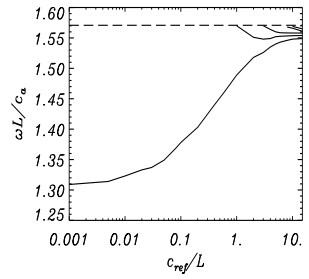

Figure 5: Logaritmic plot of the dispersion relation for a multifibril system. Adapted from [57].

for low density contrast and large inhomogeneity length-scales, the numerically calculated damping rates can deviate by up to 25% from the value predicted with the thin boundary approximation.

Recently, [70] have studied the time-dependent problem for thin and also thick boundaries. The equilibrium configuration used to model a coronal loop of radius R and length L consists of a homogeneous straight tube described in cylindrical coordinates, with ρ_i the density inside the loop, ρ_e the gas density in the loop environment ($\rho_i > \rho_e$), and l is the width of the inhomogeneous layer. The loop is permeated by a vertical and uniform magnetic field ($\mathbf{B} = B_0\mathbf{e}_z$). The Alfvén speed, $v_A = B_0/\sqrt{\mu_0\rho_0}$, takes the value v_{Ai} inside the loop and increases smoothly to the value v_{Ae} in the surrounding coronal medium (see Figure 6). Linear perturbations about this equilibrium in the zero-β limit can be readily described using the magnetohydrodynamic equations with constant resistivity

$$\frac{\partial v_r}{\partial t} = \frac{B_0}{\mu_0\rho_0}\left(-ik_z b_r - \frac{\partial b_z}{\partial r}\right), \tag{1}$$

$$\frac{\partial v_\theta}{\partial t} = \frac{B_0}{\mu_0\rho_0}\left(-ik_z b_\theta - \frac{im}{r}b_z\right), \tag{2}$$

$$\frac{\partial b_r}{\partial t} = -B_0 ik_z v_r + \eta\left(\nabla^2\mathbf{b}\right)_r, \tag{3}$$

$$\frac{\partial b_\theta}{\partial t} = -B_0 ik_z v_\theta + \eta\left(\nabla^2\mathbf{b}\right)_\theta, \tag{4}$$

$$\frac{\partial b_z}{\partial t} = -B_0\frac{1}{r}\left(v_r + r\frac{\partial v_r}{\partial r} + imv_\theta\right) + \eta\left(\nabla^2\mathbf{b}\right)_z, \tag{5}$$

where $\mathbf{v} = (v_r, v_\theta, 0)$ is the velocity and $\mathbf{b} = (b_r, b_\theta, b_z)$ is the perturbed magnetic

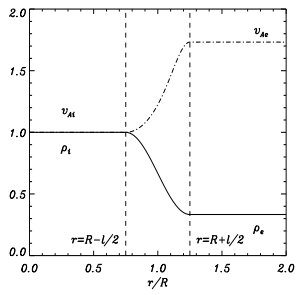

Figure 6: Dependence of the density (continuous line) and the Alfvén speed (dot-dashed line) on the radial coordinate, r. The radius of the loop is R and the width of the inhomogeneous layer is l. The vertical dashed lines mark the boundaries of the inhomogeneous layer. The density and the Alfvén speed are normalized to the value at the loop axis ($r = 0$). Distances are normalized to R. In this figure $\rho_i/\rho_e = 3$ and $l/R = 0.5$.

field. In the previous equations we have Fourier analyzed in the z-direction, i.e. we have assumed that the perturbations are of the form $e^{-ik_z z}$. We concentrate on the fundamental mode, with $k_z = \pi/L$, so the photospheric line-tying effect is automatically incorporated in the model. We impose $m = 1$, i.e. we excite the kink mode, which is the only oscillation that displaces the tube axis.

Coronal oscillations are often produced by an impulsive event and a time-dependent simulation is more appropriate to describe the evolution of the system. To study the effect of an arbitrary initial perturbation we have excited a typical loop with a disturbance located outside it. The initial perturbation induces disturbances that propagate towards the loop and also wavefronts traveling in the opposite direction. Once the perturbations reach the loop position some of the energy of the wave packet is deposited in the tube. The amount of energy deposited in the loop depends on the shape and distance of the initial perturbation from the tube. Since we are primarily interested on how the energy trapped by the loop is transferred to the inhomogeneous layer by resonant absorption, we have used an initial disturbance that deposits a considerable amount of energy in the loop. Figure 7 shows the radial velocity component, v_r, at the loop center ($r = 0$) as a function of time. We can clearly identify several phases. There are initially two large extrema followed by short-period oscillations which are quickly attenuated (see inner plot of Figure 7). After these oscillations ($t > 10\tau_A$) there is a long-period oscillation with an amplitude that attenuates in time. The short-

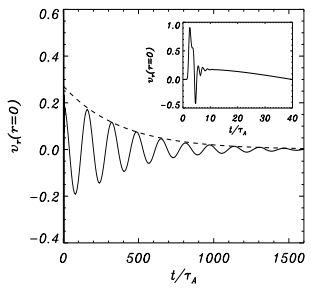

Figure 7: Plot of v_r at the center of the loop as a function of time. After a short leaky transient (for $t/\tau_A \leq 10$), detailed in the inner plot, the loop oscillates with the corresponding quasi-mode. The dashed line is a fit of the form $\exp(-t/\tau_d)$.

period oscillatory phase is related with the excitation of a leaky mode, which is a radially propagating fast wave. After the short leaky transient the loop oscillates with a much longer period. The amplitude of this mode is attenuated due to the conversion of energy from the global kink mode to the Alfvén modes. We have fitted an exponential function of the form $\exp(-t/\tau_d)$ to the envelope of the signal and have numerically determined the damping time, τ_d. It is important to point out that the resonant absorption mechanism acts very quickly (see Figure 7). Finally, it is illustrative to calculate the wave energy. Since we are in the zero-β limit there is no internal energy and there are only contributions from the kinetic and the magnetic energy,

$$E = \frac{1}{2}\left[\rho_0\left(v_r^2+v_\theta^2\right)+\frac{1}{\mu}\left(b_r^2+b_\theta^2+b_z^2\right)\right]. \quad (6)$$

A clearer signature of the resonant absorption mechanism is the transfer of energy between the global oscillation and the azimuthal Alfvénic motions. For this reason we have calculated the following energy contributions

$$E_r = \frac{1}{2}\int_0^{R+l/2}\left(\rho_0 v_r^2+\frac{1}{\mu}b_r^2\right)rdr, \quad (7)$$

$$E_\theta = \frac{1}{2}\int_0^{R+l/2}\left(\rho_0 v_\theta^2+\frac{1}{\mu}b_\theta^2\right)rdr, \quad (8)$$

$$E_z = \frac{1}{2}\int_0^{R+l/2}\frac{1}{\mu}b_z^2 rdr. \quad (9)$$

To avoid any contribution of the external medium we have computed these integrals between 0 and $R+l/2$. Note that since we have made Fourier analyses in

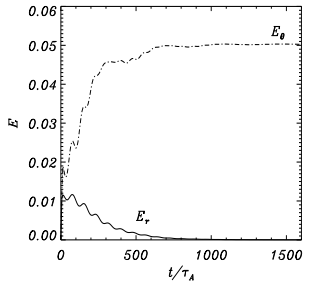

Figure 8: Integrated wave energy contributions in the region $0 < r/R < 1.25$ as a function of time. The radial energy contribution (continuous line) decreases in time while the azimuthal contribution (dot-dashed line) rises and reaches an almost constant value. The longitudinal energy contribution, E_z, is quite small in comparison with E_r and E_θ and is not represented. The impulsive leaky phase cannot be appreciated in this Figure.

the azimuthal and vertical coordinates they just contribute with a multiplicative constant to these integrals (not included in the previous expressions). Figure 8 shows the integrated energy for the case $0 < r/R < 1.25$. After the leaky transient (which lasts until $t/\tau_A \simeq 10$) the largest energy contributions are from E_r and specially from E_θ and are associated with the global motion (for a homogeneous loop $E_r = E_\theta$). The radial energy decreases quickly in time, while simultaneously the azimuthal energy increases until it reaches an almost constant value. This is a direct proof of the transfer of energy from the large scales of the global kink mode to small scales localized in the inhomogeneous layer.

3.2 Propagating slow MHD waves

Slow MHD waves propagating in coronal loops were noticed for the first time in EUV images taken with SoHO/EIT instrument [19]. Later, many observations suggesting propagating slow waves have been obtained with TRACE. In most of them, intensity disturbances start near the loop footpoints and propagate along the loop with apparent speeds (122 ± 43 km$\cdot s^{-1}$) slower than the sound speed ($c_s \approx 147$ km$\cdot s^{-1}$ in loops at temperature T = 1.0 MK). Time periods of P = 172 ± 32 s were found for loops rooted near sunspots, which coincide with the 3-minute p-mode oscillations detected in sunspots, while waves in loops rooted away from sunspots have periods of P = 321 ± 74 min, which coincide with the

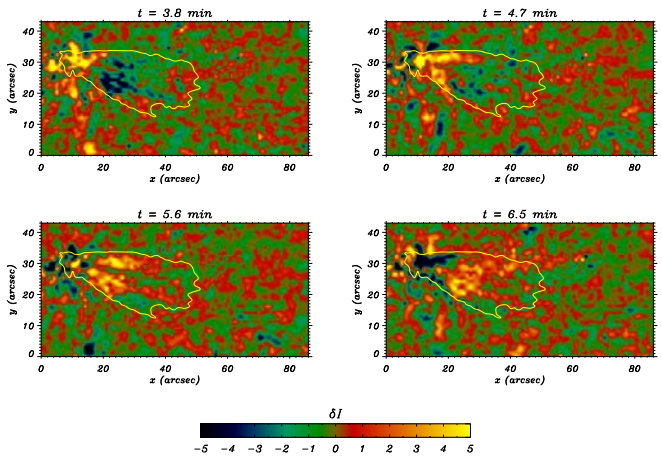

Figure 9: Four frames of the movie of the CEOF modes displaying oscillations around 5 min. The time between consecutive frames is 52.8 s $\sim$ 0.9 min. These plots clearly show the propagation of intensity fluctuations along the loop. For example, the yellow feature close to the footpoint (around position $x = 10$ and $y = 30$) in the first frame, moves along the structure and, 2.7 min later, is located around $x = 30$ and $y = 25$, as can be seen in the last frame. The yellow line delineates the edge of the loop at 07:12:38 UT.

global 5-minute p-mode oscillations. This would prove that the acoustic p-mode oscillations penetrate through the chromosphere and transition region, exciting coronal waves, however, [71] have shown that both 3 min and 5 min perturbations can coexist in the same coronal structure, so, this remains open. Basically, the properties of the propagating EUV disturbances can be summarised as follows: (a) The projected propagation speed ranges between 35 and 165 km$\cdot s^{-1}$; (b) The amplitudes are always less than 10% in intensity; (c) The disturbances are quasi-periodic with periods between $140-420$ s. The interpretation of these EUV disturbances in terms of slow magnetoacoustic waves is based in (1) The observed propagation speed agrees with the expected sound speed in the used temperature band; (2) Slow waves are compressive waves, producing a modulation of the density and EUV flux, so, observed as EUV intensity modulation. On the other hand, the wave trains were also found to fade out quickly with height probably due to the decrease of flux amplitude produced by the combined effect of the diverging geometry of the loops and thermal conduction [72, 73, 74].

Recently, [75] applied two different techniques to TRACE 171 Å intensity ob-

servations of active region AR 8496 on 1999 March 23 to obtain detailed two-dimensional information about propagating or standing waves in coronal loops. The first technique, called empirical mode decomposition (EMD), can be used to decompose a signal in its characteristic timescales, allowing, among other applications, efficient filtration of the signal. The second technique, called complex empirical orthogonal function (CEOF) analysis, is an extension of the well-known principal component analysis, to which the Hilbert transform has been added. The CEOF analysis allows identification of the dominant spatial and temporal structures in a multivariate data set and is thus ideally suited to the study of propagating and standing features that can be associated with waves or oscillations. The results indicate that a slow wave, with a period around 5 min, originates at the loop footpoint and propagates outward along the loop (see Figure 9), providing with two-dimensional information about the spatial distribution of the amplitude inside the loop. The wavelength associated to the propagating feature has been also computed giving a value of $29,000$ km while the phase velocity is approximately $100\ \mathrm{km}\cdot s^{-1}$. Since the travelling features propagate at a speed or the order of the typical coronal sound speed, which is $166\ \mathrm{km}\cdot s^{-1}$, the detected propagating feature can be interpreted as a slow magnetoacoustic wave.

4 Concluding Remarks

Coronal seismology is a rapidly developing topic which seeks to infer the internal structure and properties of coronal structures from the study of their oscillations. An extense observational background about oscillations in quiescent solar prominences, coronal loops, plumes, coronal holes, etc. has been gathered during last years. However, to make further progress coronal seismology would need new two-dimensional high-resolution observations, powerful data analysis techniques and theoretical developments which should concentrate in to perform numerical simulations in order to study the time evolution of the oscillations of equilibrium configurations as realistic as possible (inclusion of 3D, curvature, inhomogeneities, etc.) including also as much physical effects (resonant absorption, non adiabaticity, phase mixing, etc.) as possible. Once realistic configurations have been considered, the obtained results will allow a better comparison with the observations, a further refinement of the theoretical models, to obtain reliable estimations of solar corona parameters, as well as information about the contribution to the coronal heating of the different mechanisms responsible of the damping of observed oscillations.

Acknowledgements: The author would like to acknowledge the contributions to the research reported here made by M. Carbonell, A. Díaz, R. Oliver, J. Terradas and P. Forteza. The author also acknowledges financial support from MCyT under grant AYA2003-00123.

References

[1] Dyson, F. 1930, MNRAS 91, 239
[2] Moreton, G.E. 1960, AJ 65, 494
[3] Anderson, G.F. 1966, Ph. D. Thesis, University of Colorado, USA
[4] Hyder, C.L. 1966, Z. Astrophysik 63, 78
[5] Kleczek, J., Kuperus, M. 1969, Solar Phys. 6, 72
[6] Tsubaki, T. Toyoda, M., Suematsu, Y., Gamboa, Guillermo A.R. 1988, PASJ 40, 121
[7] Blanco, S., Bocchialini, K., Costa, A., Domenech, G., Rovira, M., Vial, J.C. 1999, Solar Physics 186, 281
[8] Régnier, S., Solomon, J., Vial, J.C. 2001, A&A 376, 292
[9] Pouget, G., Bocchialini, K., Solomon, J. 2006, A&A (In press)
[10] Pouget, G. 2006 (Private Communication)
[11] Oliver, R., Ballester, J.L. 2002, Solar Phys. 206, 45
[12] Terradas, J., Molowny-Horas, R., Wiehr, E., Balthasar, H., Oliver, R., Ballester, J.L. 2002, A&A 393, 637
[13] Lin, Y. 2004, Ph.D. Thesis, University of Oslo, Norway
[14] Molowny-Horas, R., Wiehr, E., Balthasar, H., Oliver, R., Ballester, J. L. 1999, in JOSO Annual Report '98, eds. A. Antalová, H. Balthasar, A. Kučera. Astronomical Institute Tatranska Lomnica, Slovakia, p.126
[15] Molowny-Horas, R., Oliver, R., Ballester, J.L., Baudin; F. 1997, Solar Phys. 172, 181
[16] Aschwanden, M.J., Fletcher, L., Schrijver, C.J., Alexander, D. 1999, ApJ 520, 880
[17] Nakariakov, V.M., Ofman, L., Deluca, E.E., Roberts, B. Davila, J.M. 1999, Science 285, 862
[18] Verwichte, E., Nakariakov, V.M., Ofman, L., Deluca, E.E. 2004, Solar Phys. 223, 77
[19] Berghmans, D., Clette, F. 1999, Solar Phys. 186, 207
[20] Nightingale, R.W., Aschwanden, M.J., Hurlburt, N.E. 1999, Sol. Phys. 190, 249
[21] De Moortel, I., Ireland, J., Walsh, R. 2000, A&A 355, L23
[22] Kliem, B., Dammasch, I.E., Curdt, W., Wilhelm, K. 2002, ApJ 568, L61
[23] Wang, T.J., Solanki, S.K., Curdt, W., Innes, D.E., Dammasch, I.E. 2002, ApJ 574, L101
[24] Roberts, B., Edwin, P.M., Benz, A.O. 1983, Nature 305, 688
[25] Roberts, B., Edwin, P.M., Benz, A.O. 1984, ApJ 279, 857
[26] Roberts, B. 2000, Solar Phys. 193, 139
[27] Roberts, B. 2004, SOHO13, ESA SP-547
[28] Aschwanden, M. 2005, Physics of the Solar Corona, Springer-Praxis

[29] Nakariakov, V.M., Verwichte, E. 2005, Living Reviews in Solar Physics 2, 3
[30] Ballester, J.L., 2006, in MHD waves and oscillations in the solar plasma, eds. R. Erdélyi, B. Roberts, M. Thompson and M. Ruderman. Phil. Trans. Royal Soc. A 364, 1839, 405
[31] Díaz, A.J., Oliver, R., Ballester, J.L. 2002, ApJ 580, 550
[32] Fasoli et a. 2002, Plasma Physics and Controlled Fusion 44, B159
[33] Ramsey, H.E., Smith, S.F. 1966, AJ 71, 197
[34] Eto, S., Isobe, H., Narukage, N., Asai, A., Morimoto, T., Thompson, B., Yashiro, S., Wang, T., Kitai, R., Kurokawa, H., Shibata, K. 2002, Pub. Astron. Soc. Japan 54, 481
[35] Okamoto, T.J., Nakai, H., Keiyama, A., Narukage, N., Ueno, S., Kitai, R., Kurokawa, H., Shibata, K. 2004, ApJ 608, 1124
[36] Jing, J., Lee, J., Spirock, T.J., Xu, Y., Wang, H., Choe, G.S. 2003, ApJ 584, L103
[37] Bashkirtsev, V.S., Mashnich, G.P. 1984, Solar Phys. 91, 93
[38] Lin, Y., Engvold, O., Van der Voort, L.R., Wiik, J.E., Berger, T. E. 2005, Solar Phys. 226, 239
[39] Yi, Z., Engvold, O. 1991, Solar Phys. 134, 275
[40] Yi, Z., Engvold, O., Keil, S. L. 1991, Solar Phys. 132, 63
[41] Engvold, O. 2001, in Proc. of Workshop on MHD Waves in Astrophysical Plasmas, eds. J.L. Ballester, B. Roberts. Universitat de les Illes Balears, p. 123
[42] Wiehr, E. 2004, in Proc. of SOHO 13 "Waves Oscillations and Small-Scale Transient Events in the Solar Atmosphere: A Joint View from SOHO and TRACE", eds. R. Erdélyi, J.L. Ballester and B. Fleck. ESA SP-547, p. 185
[43] Engvold, O.: 2005, in "Proc. IAU Colloq. on Multiwavelength Investigations of Solar Activity", eds. A.V. Stepanov, E.E. Benevolenskaya, A.G. Kosovichev. Cambridge University Press, In press.
[44] Oliver, R., Ballester, J.L., Hood, A.W., Priest, E.R. 1992, ApJ 400, 369
[45] Joarder, P.S., Roberts, B. 1992, A&A 261, 625
[46] Oliver, R., Ballester, J.L., Hood, A.W., Priest, E.R. 1993, ApJ 409, 809
[47] Poland, A., Anzer, U. 1971, Solar Phys. 19, 401
[48] Joarder, P.S., Roberts, B. 1993, A&A 277, 225
[49] Terradas, J., Carbonell, M., Oliver, R., Ballester, J.L. 2005, A&A 434, 741
[50] Díaz, A.J., Oliver, R., Erdélyi, R., Ballester, J.L. 2001, A&A 379, 1083
[51] Díaz, A.J., Oliver, R., Ballester, J.L. 2003, A&A 402, 781
[52] Ruderman, M., Roberts, B. 2002, ApJ 577, 475
[53] Khodachenko, M.L., Arber, T.D., Rucker, H.O., Hanslmeier A. 2004, A&A 422, 1073
[54] Forteza, P., Oliver, R., Ballester, J.L. 2005, A&A, In preparation
[55] Joarder, P.S., Nakariakov, V.M., Roberts, B. 1997, Solar Phys. 173, 81
[56] Joarder, P.S., Roberts, B. 1992, A&A 256, 264
[57] Díaz, A.J., Oliver, R., Ballester, J.L. 2005, A&A 440, 1167
[58] Ballester, J.L. 2003, in "Turbulence, Waves and Instabilities in the Solar Plasma", eds. R. Erdélyi, K. Petrovay, B. Roberts, M. Aschwanden). Dordrecht, p. 193
[59] Oliver, R. 2004, in Proc. of SOHO 13 "Waves Oscillations and Small-Scale Transient Events in the Solar Atmosphere: A Joint View from SOHO and TRACE", eds. R. Erdélyi, J.L. Ballester and B. Fleck. ESA SP-547, p. 175

[60] Schrijver, C.J., Title, A.M., Berger, T.E., Fletcher, L., Hurlburt, N.E., Nightingale, R.W., Shine, R.A., Tarbell, T.D., Wolfson, J., Golub, L., Bookbinder, J.A., DeLuca, E.E., McMullen, R.A., Warren, H.P., Kankelborg, C.C., Handi, B.N., De Pontieu, B. 1999, Solar Phys. 187, 261
[61] Aschwanden, M. J., De Pontieu, B., Dchrijver, C.J., Title, A.M. 2002, Solar Phys. 206, 99
[62] Nakariakov, V.M.. Ofman. L. 2001, A&A 372, L53
[63] Schrijver, C.J., Aschwanden, M.J., Title, A.M. 2002, Solar Phys. 206, 69
[64] Hudson, H.S., Warmuth, A. 2004, ApJ 614, 85
[65] Ofman. L., Aschwanden, M.J. 2002, ApJ 576, L153
[66] Heyvaerts, J., Priest, E.R. 1983, A&A 117, 220
[67] Goossens, M., Andries, J., Aschwanden, M.J. 2002, A&A 395, L39
[68] Aschwanden, M.J., Nightingale, R.W., Andries, J., Goossens, M., Van Doorsselaere, T. 2003, ApJ 598, 1375
[69] Van Doorsselaere, T., Andries, J., Poedts, S., Goossens, M. 2004, ApJ 606, 1223
[70] Terradas, J., Oliver, R., Ballester, J.L. 2006, ApJ, in press
[71] King, D.B., Nakariakov, V.M., DeLuca, E.E., Golub. L., McClements, K.G. 2003, A&A 404, L1
[72] De Moortel, I., Hood, A.W., Ireland, J. 2002, Solar Phys. 209, 89
[73] De Moortel, I., Hood, A.W. 2003, A&A 408, 755
[74] De Moortel, I., Hood, A.W. 2004, A&A 415, 704
[75] Terradas, J., Oliver, R., Ballester, J.L. 2004, ApJ 614, 435